Cell Metabolism
Short Article

Cannabinoid Receptor Type 1 Protects against Age-Related Osteoporosis by Regulating Osteoblast and Adipocyte Differentiation in Marrow Stromal Cells

Aymen I. Idris,[1] Antonia Sophocleous,[1] Euphemie Landao-Bassonga,[1] Meritxell Canals,[2] Graeme Milligan,[2] David Baker,[3] Robert J. van't Hof,[1] and Stuart H. Ralston[1,*]
[1]Rheumatic Diseases Unit, Molecular Medicine Centre, Institute of Genetics and Molecular Medicine, University of Edinburgh, Edinburgh EH4 2XU, UK
[2]Molecular Pharmacology Group, Neuroscience and Molecular Pharmacology, Faculty of Biomedical and Life Sciences, University of Glasgow, Glasgow G12 8QQ, UK
[3]Barts and the London School of Medicine and Dentistry, London E1 2AD, UK
*Correspondence: stuart.ralston@ed.ac.uk
DOI 10.1016/j.cmet.2009.07.006

SUMMARY

Age-related osteoporosis is characterized by reduced bone formation and accumulation of fat in the bone marrow compartment. Here, we report that the type 1 cannabinoid receptor (CB1) regulates this process. Mice with CB1 deficiency ($CB1^{-/-}$) had increased peak bone mass due to reduced bone resorption, but developed age-related osteoporosis with reduced bone formation and accumulation of adipocytes in the bone marrow space. Marrow stromal cells from $CB1^{-/-}$ mice had an enhanced capacity for adipocyte differentiation, a reduced capacity for osteoblast differentiation, and increased expression of phosphorylated CREB (pCREB) and PPARγ. Pharmacological blockade of CB1 receptors stimulated adipocyte differentiation, inhibited osteoblast differentiation, and increased cAMP and pCREB in osteoblast and adipocyte precursors. The CB1 receptor is therefore unique in that it regulates peak bone mass through an effect on osteoclast activity, but protects against age-related bone loss by regulating adipocyte and osteoblast differentiation of bone marrow stromal cells.

INTRODUCTION

Osteoporosis is a common disease characterized by reduced bone mineral density (BMD) and increased risk of fragility fractures. Osteoporosis becomes progressively more common with increasing age as the result of bone loss (Raisz, 2005). Women undergo a phase of rapid bone loss immediately after menopause due to estrogen deficiency, which increases bone turnover and causes uncoupling of bone resorption and bone formation (Riggs et al., 1982). Subsequently, bone turnover falls, but bone loss continues, because the amount of bone that is removed by osteoclasts exceeds that which can be replaced by osteoblasts during the bone remodeling cycle (Lips et al., 1978; Eriksen et al., 1985). This age-related reduction in osteoblast activity is due in part to the fact that bone marrow stromal cells (MSCs) from elderly subjects have a reduced capacity to differentiate into osteoblasts and an increased capacity to differentiate into adipocytes, which leads to progressive accumulation of fat in the bone marrow space with increasing age (Meunier et al., 1971; Verma et al., 2002; Justesen et al., 2001, 2002; Cao et al., 1991; Gimble et al., 2006).

Lineage commitment of MSCs is critically dependent on activation of the cyclic AMP/CREB pathway, which downregulates expression of the osteoblast-specific transcription factor Cbfa1 (Tintut et al., 1999) and upregulates expression of the adipocyte-specific transcription factors C/EBPβ and PPARγ (Cao et al., 1991; Reusch et al., 2000; Fox et al., 2006; Yang et al., 2008). Glucocorticoids, insulin, thiazolidinediones, and agents that elevate intracellular cAMP can all initiate adipogenesis in vitro, but the mechanisms by which adipogenesis is regulated in vivo remain poorly understood (Fox et al., 2006). In this study, we investigated the hypothesis that the type 1 cannabinoid receptor (CB1) might be involved in this process.

Cannabinoid receptors belong to the G protein-coupled receptor superfamily and employ Gi/o proteins to regulate cAMP levels and other intracellular signaling pathways in target cells. Cannabinoid receptor agonists such as CP55,490 bind to cannabinoid receptors and inhibit cAMP production (Demuth and Molleman, 2006), whereas antagonists such as AM251 block these effects. Most cannabinoid receptor antagonists can activate signaling in the absence of agonist binding with opposite effects on cAMP and other signaling pathways to those of agonists and hence are classified as inverse agonists (Pertwee, 1999). Recent studies have shown that both the type 1 (CB1) and type 2 (CB2) cannabinoid receptors play distinct roles in regulating bone mass and bone turnover (Idris et al., 2005, 2008b; Ofek et al., 2006), but neither receptor has been implicated in regulating osteoblast and adipocyte differentiation of MSCs. Here, we show that the CB1 pathway plays a critical role in this process and in so doing protects against age-related bone loss.

RESULTS

$CB1^{-/-}$ Mice Have Increased Peak Bone Mass, but Develop Age-Related Osteoporosis

Male and female $CB1^{-/-}$ mice had increased trabecular bone mass at 3 months, as assessed by micro-CT analysis of the tibial

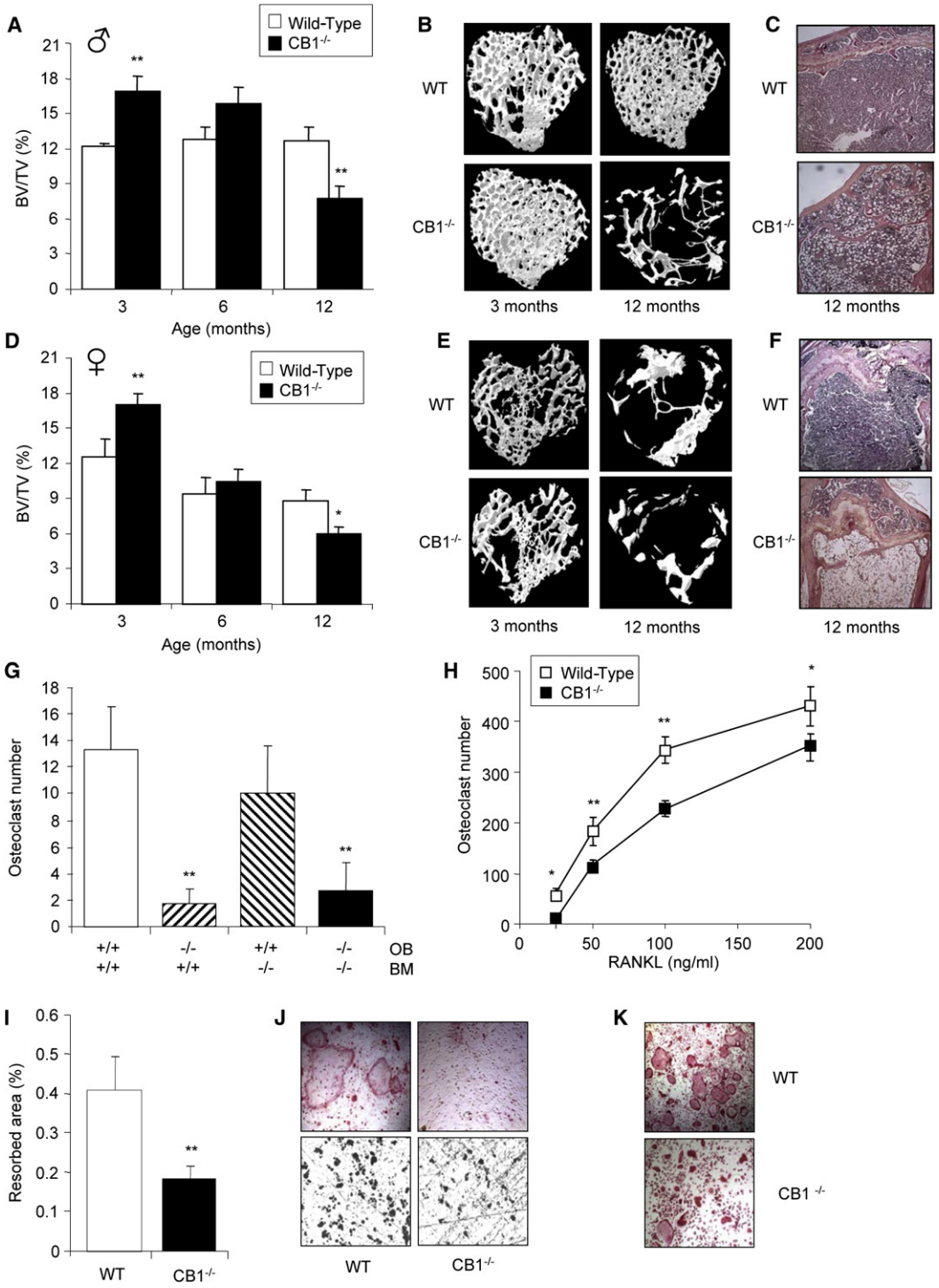

Figure 1. Mice with CB1 Deficiency Have Increased Peak Bone Mass, but Develop Age-Related Osteoporosis with Accumulation of Marrow Fat

(A) Changes in trabecular BV/TV with age in male wild-type and CB1$^{-/-}$ mice. Values are mean ± SEM from 6–8 mice per group (**p < 0.01, *p < 0.05 between genotypes).

(B) Representative micro-CT scans from 3-month-old and 12-month-old male mice.

(C) Representative photomicrographs of the tibial metaphysis from 12-month-old male mice.

(D) Changes in trabecular bone volume with age in female wild-type and CB1$^{-/-}$ mice. Values are mean ± SEM from 6–8 mice per group (**p < 0.01, *p < 0.05 between genotypes).

(E) Representative micro-CT scans from 3-month-old and 12-month-old female mice.

Table 1. Bone Histomorphometry and Biochemical Markers of Bone Turnover in CB1$^{-/-}$ and Wild-Type Mice

		Act.Res/BS (%)	Oc.N/BS (cells/mm)	Ob.N/BS (cells/mm)	Adipo/SA (%)	MAR (μm/day)	BFR/BS (μm/day)	P1NP (ng/ml)	CTX (ng/ml)
Female	Wild-type (3 months)	8.6 ± 0.8	3.5 ± 0.5	15.1 ± 1.2	0.89 ± 0.2	5.9 ± 0.2	3.5 ± 0.2	21.4 ± 1.6	36.4 ± 1.1
	CB1$^{-/-}$ (3 months)	4.1 ± 0.4***	1.6 ± 0.2*	14.0 ± 1.6	0.83 ± 0.1	6.5 ± 0.4	3.2 ± 0.4	24.5 ± 2.3	26.6 ± 3.9**
	Wild-type (12 months)	2.9 ± 3.1	0.13 ± 0.14	1.35 ± 1.1	17.6 ± 8.5	2.3 ± 0.3	1.1 ± 0.2	11.8 ± 1.1	28.8 ± 1.6
	CB1$^{-/-}$ (12 months)	0.3 ± 0.5*	0.01 ± 0.02*	0.61 ± 0.47*	76.3 ± 17.3**	1.0 ± 0.2**	0.43 ± 0.1**	6.0 ± 0.8**	25.6 ± 2.3
Male	Wild-type (3 months)	2.1 ± 0.3	0.90 ± 0.1	3.1 ± 0.3	0.55 ± 0.07	6.2 ± 0.2	3.0 ± 0.3	25.3 ± 2.5	31.4 ± 2.3
	CB1$^{-/-}$ (3 months)	0.8 ± 0.07**	0.30 ± 0.04*	2.8 ± 0.4	0.67 ± 0.01	6.7 ± 0.3	2.5 ± 0.3	21.8 ± 0.9	23.7 ± 2.1**
	Wild-type (12 months)	0.7 ± 0.1	0.30 ± 0.07	1.8 ± 0.4	2.66 ± 0.8	4.6 ± 0.3	1.9 ± 0.3	10.6 ± 0.4	27.8 ± 2.8
	CB1$^{-/-}$ (12 months)	0.08 ± 0.01*	0.02 ± 0.01*	0.7 ± 0.1**	56.8 ± 19.3**	1.3 ± 0.1**	0.56 ± 0.08**	4.9 ± 0.6**	18.8 ± 1.6**

Values are means ± SEM and are obtained from 6–8 animals per group, with the exception of P1NP in 12-month-old wild-type mice, where only 4 samples were available for analysis (* $p < 0.05$, ** $p < 0.01$, *** $p < 0.001$, wild-type versus CB1$^{-/-}$ mice of the same age).
Act.Res/BS, active resorption surface/bone surface; Oc.N/BS, osteoclast number/bone surface; Ob.N/BS, osteoblast number/bone surface; Adipo/SA, adipocyte area/section area; MAR, mineral apposition rate; BFR/BS, bone formation rate/bone surface.

metaphysis, when compared with wild-type littermates (Figures 1A–1E). Bone histomorphometry showed that active resorption surface and osteoclast numbers were significantly reduced in male and female CB1$^{-/-}$ mice at this age when compared with wild-type, whereas no differences were observed in osteoblast number, mineral apposition rate (MAR), or bone formation rate (BFR) (Table 1). In keeping with these observations, serum levels of the bone resorption marker C-terminal telopeptide crosslinks (CTX) were reduced in 3-month-old CB1$^{-/-}$ mice compared with wild-type, whereas levels of the N-terminal propeptide of type 1 procollagen (P1NP), a bone formation marker, were not significantly different (Table 1). These findings indicate that the likely mechanism for the increased trabecular bone mass in CB1$^{-/-}$ mice is a relative reduction in osteoclast activity in the face of normal osteoblast activity, causing a positive balance in favor of bone formation during skeletal growth. In order to define the mechanisms responsible for the reduced osteoclast activity, we studied osteoclast differentiation in CB1$^{-/-}$ mice and wild-type controls using osteoblast-bone marrow cocultures and receptor activator of nuclear factor kappa B ligand (RANKL)-stimulated bone marrow macrophage cultures. Osteoclast formation was significantly reduced in cocultures prepared from CB1$^{-/-}$ mice when compared with wild-type mice, but this was largely rescued by culture of CB1$^{-/-}$ marrow cells with wild-type osteoblasts (Figure 1G). This indicates that CB1 deficiency impairs the ability of osteoblasts to support osteoclast formation. Since osteoclast formation is critically dependent on RANKL expressed by osteoblasts (Kong et al., 1999), we studied RANKL expression by quantitative PCR in osteoblast cultures and found that RANKL mRNA levels were significantly lower in CB1$^{-/-}$ cultures than in wild-type cultures (1584 ± 117 copies versus 2041 ± 140 copies; $p < 0.01$). Resorption pit formation was also reduced in cocultures from CB1$^{-/-}$ mice as compared with wild-type (Figure 1I), in keeping with the reduction in osteoclast numbers (representative photomicrographs, Figure 1J). We also found that RANKL- and macrophage colony stimulating factor (M-CSF)-induced osteoclast formation was reduced in bone marrow macrophage cultures from CB1$^{-/-}$ mice as compared with wild-type (Figure 1H; representative photomicrographs, Figure 1K). Taken together, these observations demonstrate that CB1 regulates osteoclast differentiation both directly, by negatively impacting on the ability of osteoclast precursors to respond to M-CSF and RANKL, and indirectly, by modulating expression of RANKL by osteoblast-like cells.

Although CB1$^{-/-}$ mice of both genders had increased trabecular bone mass at 3 months of age when compared with wild-type, they developed osteoporosis with increasing age (Figures 1A–1F). In male CB1$^{-/-}$ mice, trabecular bone volume/tissue volume (BV/TV) fell by a mean (± SEM) of 54% ± 6.3% compared with a 3.7% ± 10.1% gain in wild-type littermates ($p < 0.001$). Similarly, BV/TV fell by 64.6% ± 3.7% in female CB1$^{-/-}$ mice compared with a 37.1% ± 9.4% fall in wild-type littermates ($p < 0.01$). Analysis of trabecular bone by micro-CT at lumbar vertebra 5 showed a pattern similar to that observed at the tibial metaphysis, with higher BV/TV values at 3 months in CB1$^{-/-}$ mice, but lower values at 12 months (data not shown). Histological analysis of the tibial metaphysis in 12-month-old mice showed that the osteoporosis in CB1$^{-/-}$ mice was associated with a striking increase in accumulation of adipocytes in the bone marrow compartment (Figures 1C and 1F). This was particularly evident in females, where the bone marrow space was almost completely replaced with adipocytes. Analysis of bone histomorphometry in 12-month-old mice showed evidence of reduced bone turnover in both CB1$^{-/-}$ and wild-type, but

(F) Representative photomicrographs of the tibial metaphysis from 12-month-old female mice.
(G) Bone marrow osteoblast cocultures in CB1$^{-/-}$ and wild-type mice. Values are mean ± SEM and are representative of three independent experiments (** $p < 0.01$ from wild-type cultures).
(H) RANKL- and M-CSF-generated osteoclast formation from CB1$^{-/-}$ and wild-type mice. Values are mean ± SEM and are representative of three independent experiments (** $p < 0.01$, * $p < 0.05$ between genotypes).
(I) Resorption pit formation in bone marrow osteoblast cocultures from CB1$^{-/-}$ and wild-type mice. Values are mean ± SEM and are representative of three independent experiments (** $p < 0.01$, between genotypes).
(J) Photomicrographs of dentine slices from cocultures in CB1$^{-/-}$ and wild-type mice.
(K) Representative photomicrographs of osteoclast cultures from CB1$^{-/-}$ and wild-type mice.

osteoclast numbers, active resorption surfaces, osteoblast number, MAR, and BFR were all significantly lower in CB1$^{-/-}$ compared with wild-type, and adipocyte area was greatly increased (Table 1). Serum levels of P1NP and CTX were also lower in CB1$^{-/-}$ mice compared with wild-type at 12 months, but the difference between genotypes was not statistically significant for CTX in female mice. These data demonstrate that the age-related osteoporosis in CB1$^{-/-}$ mice of both genders is associated with low turnover with a reduction in bone formation and accumulation of bone marrow fat.

The CB1 Pathway Regulates Osteoblast and Adipocyte Differentiation in Bone MSCs

In order to investigate the mechanisms underlying the reduced bone formation and increased fat accumulation in CB1$^{-/-}$ mice, we studied osteoblast and adipocyte differentiation in MSC cultures prepared from CB1$^{-/-}$ and wild-type mice. MSCs from CB1$^{-/-}$ mice had a significantly reduced capacity to form mineralized bone nodules when cultured in osteogenic medium (Figures 2A and 2B). Similar results were obtained whether the cultures were performed using cells derived from 3-, 6-, and 12-month old mice (data not shown). Bone nodule formation was inhibited by pharmacological blockade of CB1 receptors with AM251 (Figures 2C and 2D), but was stimulated by CP55,490, a nonselective cannabinoid receptor agonist (Figures 2E and 2F). Further studies showed that CB1$^{-/-}$ MSCs had an enhanced ability to differentiate into adipocytes when cultured in adipogenic medium (Figures 2G and 2H) and showed increased expression of the adipogenic transcription factors PPARγ and phosphorylated cAMP response element-binding factor (pCREB) compared with wild-type (Figure 2I). Moreover, the stimulatory effect of AM251 on adipocyte differentiation could be reversed by the cannabinoid receptor agonist CP55,490 and the Gi/o inhibitor pertussis toxin (Figures 2J and 2K). Taken together, these data indicate that signaling through the CB1 receptor regulates the ability of bone MSCs to differentiate into adipocytes in vitro and are consistent with a model whereby deficiency of CB1 predisposes to osteoporosis by reciprocally regulating adipocyte and osteoblast differentiation in the bone marrow compartment in vivo.

Cannabinoid Ligands Regulate cAMP and CREB in Preadipocytes and Osteoblast-like Cells

Since cAMP and CREB play important roles in regulating adipocyte differentiation in vitro (Fox et al., 2006), we wanted to determine if CB1 signaling modulates cAMP and CREB phosphorylation in preadipocytes and osteoblast-like cells. The cannabinoid receptor agonist CP55,490 inhibited forskolin-induced cAMP accumulation in 3T3-L1 preadipocytes, and this was reversed by AM251 and the Gi/o inhibitor pertussis toxin (Figure 3A). Further studies showed that AM251 increased pCREB in 3T3-L1 cells, but had no effect on levels of the related transcription factor ATF1 and no consistent effect on total CREB (Figure 3B). In MC3T3 cells, we observed similar effects of CP55,490, pertussis toxin, and AM251 on cAMP levels (Figure 3C) and found that AM251 increased pCREB and, to a lesser extent, ATF-1, but had no effect on total CREB (Figure 3D). Taken together, these data indicate that signaling through the CB1 receptor regulates cAMP levels and CREB phosphorylation in preadipocytes and osteoblast-like cells, providing an explanation for the enhancement of adipocyte differentiation and reduction in bone nodule formation, which we observed in MSC cultures from CB1$^{-/-}$ mice.

Expression of CB1 in the Bone Microenvironment Increases with Age

While CB1 is highly expressed in the brain, it is also widely expressed in peripheral tissues (Howlett et al., 2002). Since the in vitro studies that we performed showed that CB1 exerts direct effects on bone cells, we studied levels of CB1 expression in the bone microenvironment by quantitative PCR and looked for evidence of possible changes in CB1 expression with age in view of the dramatic effect of age on the skeletal phenotype in CB1$^{-/-}$ mice. These studies showed that the mRNA levels for CB1 were highest in the brain, but were also clearly detectable in several other cell types in the periphery, including MSCs, osteoblasts, osteoclasts, bone marrow macrophages, spleen, and adipocytes (Figure 3E). There also was a significant increase in levels of CB1 transcript between 3 and 12 months of age in freshly isolated bone marrow cells from wild-type mice (Figure 3F), demonstrating that CB1 expression is upregulated with age in the bone marrow compartment, providing a possible explanation for the age-related effects of CB1 deficiency on bone loss and marrow fat accumulation.

DISCUSSION

The observations presented here demonstrate that the CB1 pathway plays a unique role in bone metabolism by regulating peak bone mass through effects on osteoclastogenesis and bone resorption and age-related bone loss through effects on differentiation of MSCs. Mice with CB1 deficiency had significantly increased trabecular bone mass at 3 months of age when compared with wild-type littermates, and levels of osteoclastic bone resorption were reduced. Bone marrow macrophages from CB1$^{-/-}$ mice were less responsive to RANKL and M-CSF than wild-type, and CB1$^{-/-}$ osteoblasts were less able to support osteoclast formation and expressed lower amounts of RANKL. Since bone formation in 3-month-old CB1$^{-/-}$ mice was similar to that of wild-type, this indicates that the high trabecular bone mass that we observed was primarily due to a reduction in bone resorption in the presence of normal bone formation. The high peak bone mass reported here is in keeping with the findings of Tam and colleagues, who reported that 3-month-old CB1$^{-/-}$ mice on a CD1 genetic background had high trabecular bone mass, although the difference was statistically significant only for males (Tam et al., 2008). It should be noted, however, that in Tam's study, CB1$^{-/-}$ mice on a C57BL/6 background were found to have low bone mass. The reason for the difference between strains is unclear, although it might be partly related to the fact that, among common inbred strains, C57BL/6 mice have the lowest femoral volumetric bone density and femoral trabecular bone volume (Beamer et al., 1996). It could be that C57BL/6 mice harbor recessive mutations in pathways that abrogate or modify the effects of the CB1 pathway on bone cell activity or that CB1$^{-/-}$ mice on a CD1 background have a distinct skeletal phenotype because of epistatic interactions with polymorphisms in other genes.

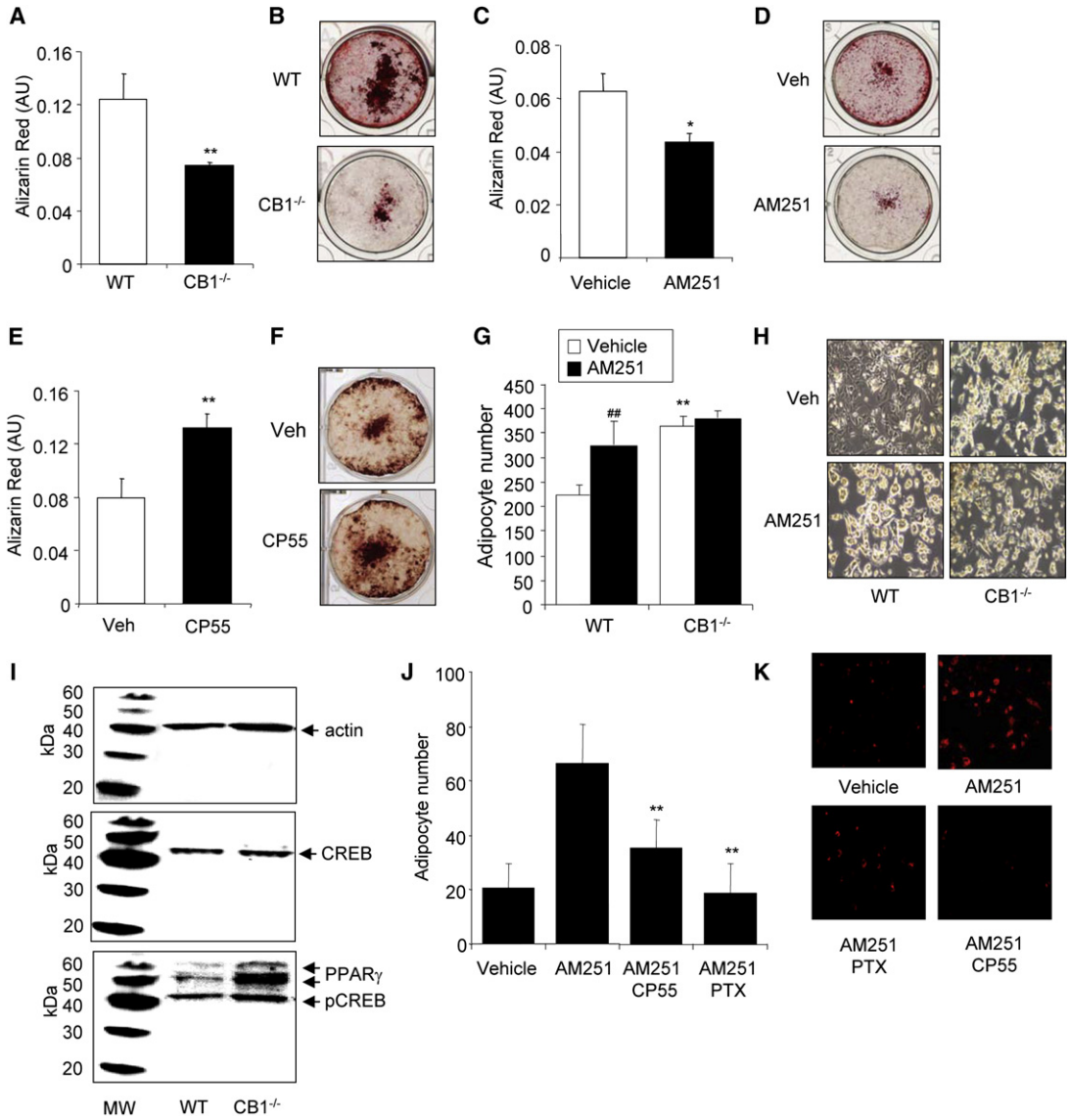

Figure 2. The CB1 Pathway Regulates Osteoblast and Adipocyte Differentiation In Vitro

(A) Bone nodule formation in MSC cultures from CB1$^{-/-}$ and wild-type mice. Values are mean ± SEM and are representative of three independent experiments (**$p < 0.01$ between genotypes).

(B) Representative photomicrographs from the cultures shown in (A).

(C) Bone nodule formation in MSC cultures from wild-type mice in the presence or absence of AM251 (100 nM). Values are mean ± SEM and are representative of three independent experiments (**$p < 0.01$ between genotypes).

(D) Representative photomicrographs from the cultures shown in (C).

(E) Bone nodule formation in MSC cultures from wild-type mice in the presence or absence of CP55,490 (CP55; 100 nM). Values are mean ± SEM and are representative of three independent experiments (**$p < 0.01$ between genotypes).

(F) Representative photomicrographs from the cultures shown in (E).

(G) Adipocyte formation in MSC cultures from CB1$^{-/-}$ and wild-type mice grown in adipogenic medium in the presence and absence of AM251 (100 nM). Values are means ± SEM and are representative of at least three independent experiments (**$p < 0.01$ between genotypes; $^{\#\#}p < 0.01$ vehicle versus AM251).

(H) Representative photomicrographs from the cultures shown in (G). Adipocytes are the cells with accumulation of yellow/white lipid droplets in the cytoplasm.

(I) Expression of PPARγ and pCREB in the cultures shown in (G), assessed by western blotting.

(J) Adipocyte formation in wild-type MSCs cultured in adipogenic medium stained with Nile red O and treated with AM251, pertussis toxin (PTX; 20 ng/ml), and CP55,490.

(K) Representative photomicrographs from the cultures shown in (J).

While peak bone mass was initially higher in CB1$^{-/-}$ mice, greater amounts of bone were lost with increasing age when compared with wild-type. Accordingly, levels of trabecular bone mass were similar in 6-month-old CB1$^{-/-}$ mice and wild-type controls, whereas by 12 months, CB1$^{-/-}$ mice had developed marked osteoporosis, with replacement of the bone

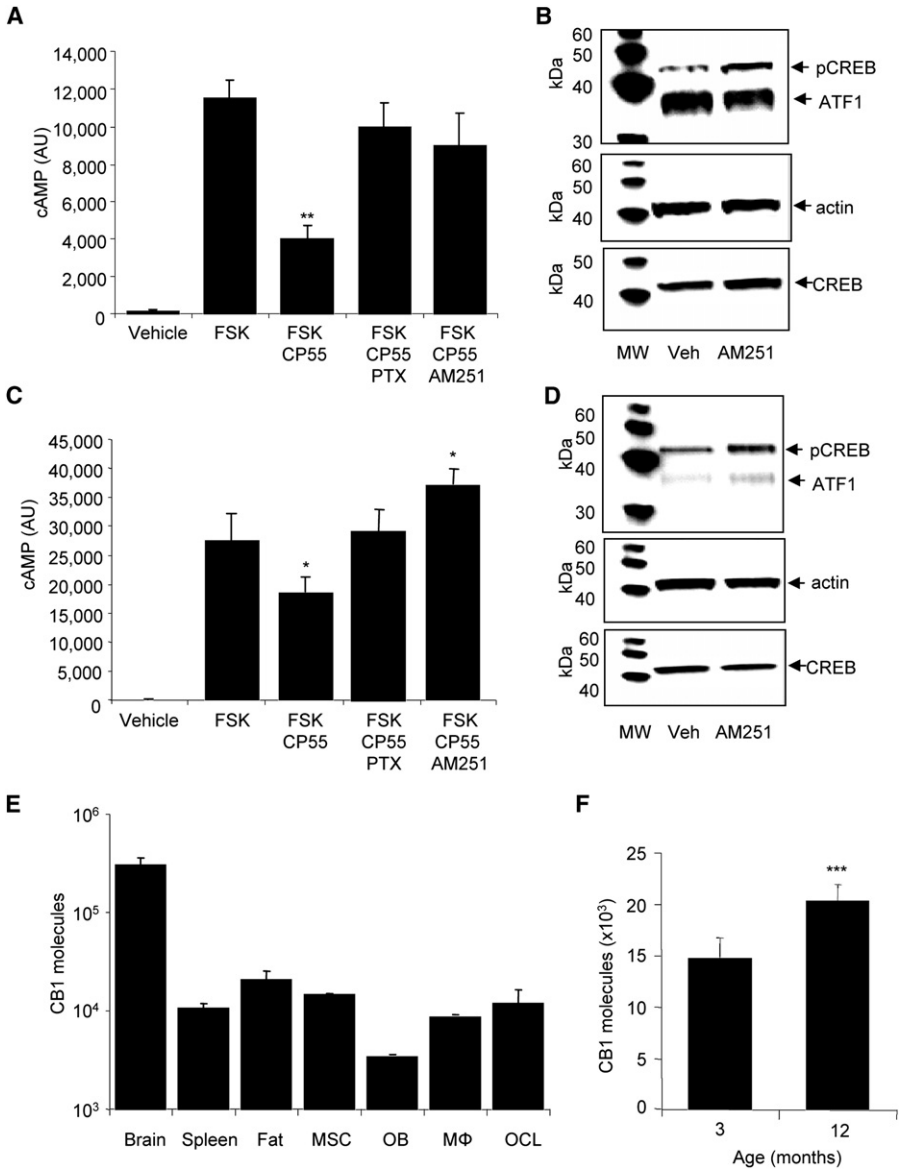

Figure 3. Cannabinoids Regulate cAMP Signaling and CREB Phosphorylation in Adipocytes and Osteoblasts

(A) Effects of CP55,490 (CP55; 100 nM), AM251 (100 nM), forskolin (FSK; 10 μM), and pertussis toxin (PTX; 20 ng/ml) on cAMP levels in 3T3-L1 preadipocytes. Levels of cAMP are in arbitrary units derived from incorporation of [^{3}H] to cAMP in relation to total [^{3}H]adenine-containing nucleotides. Values are mean ± SEM and are representative of three independent experiments (**$p < 0.01$, FSK versus other groups).

(B) Effect of AM251 on total CREB, pCREB, and ATF1 in 3T3-L1 preadipocyte cultures, assessed by western blotting.

(C) Effects of CP55,490 (CP55; 100 nM), AM251 (100 nM), forskolin (FSK; 10 μM) and pertussis toxin (PTX; 20 ng/ml) on cAMP levels in MC3T3 osteoblast-like cells. Level of cAMP are in arbitrary units derived from incorporation of [^{3}H] to cAMP in relation to total [^{3}H]adenine-containing nucleotides. Values are mean ± SEM and are representative of three independent experiments (*$p < 0.05$, FSK versus other groups).

(D) Effect of AM251 on total CREB, pCREB, and ATF1 in MC3T3 osteoblast-like cell, assessed by western blotting.

(E) Expression of CB1 mRNA assessed by quantitative PCR and expressed as the number of molecules per nanogram of total RNA in various cells and tissues.

(F) Expression of CB1 mRNA in freshly isolated bone marrow cells from mice aged 3 and 12 months (***$p < 0.01$ between groups; MSC, bone marrow stromal cell; OB, osteoblast; MΦ, macrophage; OCL, osteoclast).

marrow compartment by adipocytes. This was particularly evident in females, but was also observed in males. Histomorphometric analysis showed that levels of bone turnover were reduced at 12 months of age when compared with 3 months in both CB1$^{-/-}$ and wild-type mice, but the reduction in bone formation was significantly greater in CB1$^{-/-}$ mice when compared with wild-type. Although histomorphometric indices of bone resorption were also lower in 12-month-old CB1$^{-/-}$ mice as compared with wild-type, the reduction in bone formation was clearly more profound than the reduction in bone resorption, reflected by the fact that both male and female CB1$^{-/-}$ mice developed osteoporosis with increasing age.

In keeping with the findings in vivo, we found that MSCs from CB1$^{-/-}$ mice had an impaired ability to differentiate into osteoblasts, but an increased ability to differentiate into adipocytes in vitro. These differences in lineage commitment were accompanied by reduced expression of Cbfa1, which promotes osteoblast differentiation, and increased expression of pCREB and PPARγ, which promote adipocyte differentiation. Raised intracellular levels of cAMP are known to stimulate adipocyte differentiation in vitro by promoting CREB phosphorylation, which in turn increases expression of the adipocyte-specific transcription factors C/EBPβ, PPARγ, and C/EBPα (Fox et al., 2006; Yang et al., 2008). Conversely, increased levels of cAMP in preosteoblasts inhibit osteoblast differentiation by reducing Cbfa1 expression and Cbfa1-DNA binding (Tintut et al., 1999). In this study, the cannabinoid receptor agonist CP55,490 inhibited forskolin-induced cAMP accumulation in 3T3-L1 cells, and this effect was reversed by the CB1 selective inverse agonist AM251 and the Gi/o inhibitor pertussis toxin. Moreover, the stimulatory effect of AM251 on adipocyte differentiation of mesenchymal stem cells was abrogated by pertussis toxin, which is known to block receptor-mediated regulation of the Gi/o protein (Yajima et al., 1986), illustrating that CB1 regulates adipocyte differentiation by a Gi/o-mediated pathway. Similar responses were observed in MC3T3 osteoblast-like cells, suggesting that CB1 also regulates osteoblast differentiation by a cAMP-dependent pathway. Taken together, these observations are consistent with a model whereby CB1 deficiency increases cAMP levels in mesenchymal stromal cells, leading to CREB phosphorylation and increased PPARγ expression, thereby enhancing adipocyte differentiation at the expense of osteoblast differentiation. In accordance with this view, the skeletal phenotype observed in aged CB1$^{-/-}$ mice was, in many respects, similar to that reported in mice that have been treated with rosiglitazone, which directly activates PPARγ to increase adipocyte differentiation and inhibit osteoblast differentiation (Ali et al., 2005; Rzonca et al., 2004).

It is of interest that the reduced bone formation and increased marrow fat accumulation was observed only in aged CB1$^{-/-}$ mice, even though MSCs cultured from CB1$^{-/-}$ mice of all ages had a reduced ability to differentiate into osteoblasts and an increased ability to differentiate into adipocytes in vitro. This suggests that in young mice, other signaling pathways can compensate for the effects of CB1 deficiency in vivo and maintain normal bone formation. With increasing age, however, these compensatory mechanisms clearly fail, leading to the defect in bone formation and increase in marrow fat accumulation that we observed in aged mice. Further research will now be required to identify these pathways and the mechanisms by which they interact with CB1 deficiency to influence MSC differentiation in vivo. One such factor might be levels of CB1 expression, since we observed a 25% increase in CB1 expression in bone marrow of wild-type mice between 3 and 12 months, raising the possibility that there is physiological upregulation of CB1 expression with age, which protects against the development of osteoporosis.

Since the CB1 receptor is known to play a role in energy metabolism, we considered the possibility that the changes in marrow fat distribution might have been related to generalized changes in fat metabolism. In this regard, previous studies have shown that CB1$^{-/-}$ mice are leaner than wild-type controls, due in part to the fact that they eat less (Ravinet et al., 2004). The CB1$^{-/-}$ mice used in this study had a 3%–7% lower body weight than wild-type controls, but these differences were constant throughout life (data not shown). Although we cannot completely exclude the possibility that redistribution of adipocytes from peripheral sites to the bone marrow space might have occurred, this would not explain the reduction in bone formation that we observed in 12-month-old CB1$^{-/-}$ mice or the effects of CB1 on adipocyte and osteoblast differentiation in vitro.

The stimulatory effect of CB1 on osteoblast differentiation that we found in this study is in keeping with the observations made by Tam and colleagues, who reported that CB1 acts as a mediator of increased bone formation that follows traumatic brain injury (TBI) (Tam et al., 2008). In that study, TBI-induced bone formation was absent in CB1$^{-/-}$ mice and was also blocked by isoprenaline infusions. This led the authors to speculate that CB1 stimulates bone formation by inhibiting release of catecholamines from peripheral nerves, although in the present study, we observed direct effects of CB1 on osteoblast differentiation in vitro. While we cannot exclude the possibility that CB1-regulated neurogenic pathways may have contributed to the phenotype that we observed, the present study shows that CB1 exerts cell-autonomous effects on differentiation of mesenchymal cells to osteoblasts and adipocytes and exerts direct effects on osteoclast differentiation. Further studies using cell-specific or neuron-specific inactivation of CB1 will be required to address the relative importance of central versus peripheral CB1 signaling to the regulation of the skeletal phenotypes described in this study.

In summary, our studies demonstrate that CB1 plays a unique role in bone metabolism by exerting bidirectional effects on bone mass at different stages in life, by modulating osteoclast differentiation, and by regulating differentiation of MSCs into osteoblasts and adipocytes. This work has important clinical implications in raising the possibility that cannabinoid receptor ligands may be of value therapeutically in enhancing peak bone mass and in preventing age-related osteoporosis, but indicates that agonists and antagonists may exert contrasting effects on the skeleton at different stages in life.

EXPERIMENTAL PROCEDURES

Materials

All reagents were obtained from Sigma (Poole Dorset, UK) unless otherwise indicated. Culture media were obtained from Invitrogen (Paisley, UK), and antibodies were from Cell Signaling Technology (Danvers, MA), unless otherwise stated. Cultures were grown in α-MEM supplemented with 10% FCS, 1% penicillin, 1% streptomycin, and 2 mM glutamine. The cannabinoid receptor ligands AM251 and CP55,490 were obtained from Tocris Bioscience (Bristol, UK), dissolved in DMSO, and added to the cell cultures in the concentrations indicated such that the final concentration of DMSO was 0.1% or less. Control cultures were treated with DMSO alone at the same concentration.

Animals

Mice with targeted inactivation of CB1 were generated by homologous recombination as described previously (Ledent et al., 1999) and were a kind gift from Dr. Christine Ravinet-Trillou (Sanofi-Aventis; Paris). Heterozygous mice were bred for at least 17 generations onto a CD1 background before generating the CB1$^{-/-}$ and wild-type littermates used in this study.

Osteoblast Isolation and Culture

Osteoblasts were isolated from the calvarial bones of 2-day-old mice by sequential collagenase digestion. Prior to experimentation, the cells were

cultured into a 75 cm^2 flask in standard α-MEM and left to adhere overnight. Osteoblasts were then seeded onto 96-well plates at 8 × 10^3 cells per well, 48-well plates at 12 × 10^3 cells per well, or 12-well plates at 60 × 10^3 cells per well. Osteoblast numbers were determined by Alamar blue assay according to the manufacturer's instruction. Subsequently, cell extracts were prepared, and alkaline phosphatase activity was measured and corrected for cell number previously described (Idris et al., 2008a).

Bone Nodule and Adipocyte Cultures

MSCs from female CB1$^{-/-}$ and wild-type mice were seeded into 12-well plates at 60 × 10^3 cells per well in 2 ml of α-MEM supplemented with 3 mM β-glycerol phosphate and 50 μg/ml L-ascorbic acid as previously described (Idris et al., 2008a). The cells were cultured for between 10 and 21 days, with replacement of the culture medium every 3 days and daily replacement of L-ascorbic acid. At the end of the cultures, the plates were fixed in 70% cold ethanol, and the mineralized nodules were visualized by alizarin red staining. Bone nodule formation was quantitated by destaining the cultures for 15 min in cetylpyridinium chloride and measuring absorbance of the extracted stain by spectrophotometry as previously described (Stewart et al., 2005). The values were normalized to cell number as determined by the Alamar blue assay. For the primary adipocyte cultures, marrow cells were isolated from the long bones of 3- to 5-month-old mice and seeded into a Petri dish at 1 × 10^8 cells in 10 ml of standard α-MEM supplemented with insulin (10 mg/ml), with replacement of the culture medium every 2 days until confluence. Adherent cells were released with trypsin and replated at 10^4 cells/well in 24-well plates in 500 μl culture medium supplemented with insulin (10 μg/ml), dexamethasone (250 nM), indomethacin (100 nM), troglitazone (1 μM), and isobutylmethylxanthine (0.5 μM) for 2–4 days in the presence or absence of test factors. At the end of the culture period, adipocytes were identified morphologically by Nile red O staining and quantitated by counting six high-powered fields per treatment group. For the preadipocyte 3T3-L1 cultures, cells were seeded into 12-well tissue culture plates at 1 × 10^5 cells in 1 ml of standard α-MEM supplemented with insulin (1 μg/ml), with replacement of the culture medium every 2 days until confluence.

Bone Marrow Cocultures and Osteoclast Cultures

Bone marrow cells were isolated from the long bones of 3- to 5-month-old mice and seeded into a Petri dish at 1 × 10^8 cells in 10 ml of standard α-MEM. The adherent stromal cells were trypsinized and replated together with the nonadherent bone marrow cells at 10^4 cells/well and 2 × 10^5 cells/well, respectively, on dentine slices in 96-well plates in 150 μl of standard α-MEM supplemented with 10 nM 1,25-dihydroxyvitamin D_3 for 10 days. For the RANKL-generated osteoclast cultures, nonadherent bone marrow cells were cultured in the presence of 100 ng/ml M-CSF (R&D Systems; Abingdon, UK) for 2 days followed by another 3 days in the presence of 25 ng/ml M-CSF (R&D Systems) and 100 ng/ml RANKL (a gift from Patrick Mollat, Galapagos; Romaineville, France), so the total culture time was 5 days. Osteoclasts were identified by TRAcP staining as described previously (van't Hof, 2003).

Western Blotting

Cells lysates were prepared using a buffer containing 100 mM Tris-HCl (pH 7.8), 150 mM NaCl, 0.1% Triton X-100, 5% protease inhibitor cocktail, and 5% phosphatase inhibitor cocktail. Protein content was determined, and an identical amount of protein from each extract was analyzed by SDS-PAGE and transferred to a PVDF membrane (Amersham Biosciences; Amersham, UK). Levels of PPARγ and pCREB were detected using a rabbit monoclonal anti-PPARγ antibody and a rabbit monoclonal anti-pCREB antibody and normalized to actin expression using a polyclonal anti-β-actin antibody (all at 1:1000 dilution). Subsequently, the membranes were incubated with the appropriate secondary antibodies coupled to horseradish peroxidase (1:10000 dilution), and the bands were visualized using chemiluminescence (Amersham Biosciences) on a BioRad Fluomax gel imaging system.

Adenylyl Cyclase Measurements

Measurements of adenylyl cyclase activity were performed as described (Merkouris et al., 1997). The cells were cultured in poly-D-lysine-coated 12-well plates and incubated in medium containing [^{3}H]adenine (1.5 μCi/well) for 16 hr. Generation of [^{3}H]cAMP in response to the treatment was assessed by chromatography. Results are presented as the ratio of levels of [^{3}H]cAMP to total [^{3}H]adenine nucleotides.

Quantitative PCR

Cells and tissues were lysed using TRIzol reagent, and the RNA was recovered by precipitation with isopropyl alcohol. The pellet was washed with 70% ethanol and suspended in DEPC-treated water. RNA was quantified using a RiboGreen dye kit (Invitrogen), and complementary DNA (cDNA) was generated using the SuperScript III Reverse Transcriptase kit (Invitrogen). The product was cleaned using a PCR purification kit (Invitrogen) and visualized on a 1.5% agarose gel stained with SYBR green dye adjacent to a low-molecular-weight ladder. Primers were designed using the Ensembl Genome Browser and the Roche website (Roche; Burgess Hill, UK). Copies of the primer and probe sequences are available from the authors on request. Levels of gene expression were expressed as copy number per nanogram of total RNA.

Bone Histomorphometry and Micro-CT Analysis

Bone histomorphometry was performed on the proximal tibial metaphysis. The bones were fixed in 70% ethanol, decalcified in 10% EDTA, and embedded in methyl-methacrylate using the Technovit 9100 kit (TAAB; Reading, UK) or in wax sections, according to standard techniques. Sections were prepared using a Leica microtome (1.5 μm thick for MMA and 5 μm thick for wax), and bone histomorphometry was assessed using a semiautomated image analysis system. Micro-CT analysis was performed at the left tibial metaphysis (200 slices directly distal of the growth plate) using a SkyScan 1172 instrument set at 60 kV and 150 μA, at a resolution of 5 μm. The images were reconstructed using the SkyScan NRecon program and analyzed using SkyScan CTAn software.

Biochemical Markers of Bone Turnover

Serum CTX (a marker of bone resorption) and P1NP (a marker of bone formation) were measured using mouse/rat competitive enzyme immunoassay kits (IDS; Boldon, UK), according to the manufacturer's instructions.

ACKNOWLEDGMENTS

This study was supported by an integrated clinical arthritis centre grant (17687) and a program grant (17713) from the Arthritis Research Campaign (UK). A.I.I. is partly supported by a European Calcified Tissues Society Amgen Fellowship, and A.S. is supported by a University of Edinburgh PhD studentship. The authors report that they have no conflicts of interest.

Received: January 5, 2009
Revised: May 4, 2009
Accepted: July 20, 2009
Published: August 5, 2009

REFERENCES

Ali, A.A., Weinstein, R.S., Stewart, S.A., Parfitt, A.M., Manolagas, S.C., and Jilka, R.L. (2005). Rosiglitazone causes bone loss in mice by suppressing osteoblast differentiation and bone formation. Endocrinology *146*, 1226–1235.

Beamer, W.G., Donahue, L.R., Rosen, C.J., and Baylink, D.J. (1996). Genetic variability in adult bone density among inbred strains of mice. Bone *18*, 397–403.

Cao, Z., Umek, R.M., and McKnight, S.L. (1991). Regulated expression of three C/EBP isoforms during adipose conversion of 3T3-L1 cells. Genes Dev. *5*, 1538–1552.

Demuth, D.G., and Molleman, A. (2006). Cannabinoid signalling. Life Sci. *78*, 549–563.

Eriksen, E.F., Mosekilde, L., and Melsen, F. (1985). Trabecular bone resorption depth decreases with age: differences between normal males and females. Bone *6*, 141–146.

Fox, K.E., Fankell, D.M., Erickson, P.F., Majka, S.M., Crossno, J.T., Jr., and Klemm, D.J. (2006). Depletion of cAMP-response element-binding protein/ATF1 inhibits adipogenic conversion of 3T3-L1 cells ectopically expressing

CCAAT/enhancer-binding protein (C/EBP) alpha, C/EBP beta, or PPAR gamma 2. J. Biol. Chem. *281*, 40341–40353.

Gimble, J.M., Zvonic, S., Floyd, Z.E., Kassem, M., and Nuttall, M.E. (2006). Playing with bone and fat. J. Cell. Biochem. *98*, 251–266.

Howlett, A.C., Barth, F., Bonner, T.I., Cabral, G., Casellas, P., Devane, W.A., Felder, C.C., Herkenham, M., Mackie, K., Martin, B.R., et al. (2002). International Union of Pharmacology. XXVII. Classification of cannabinoid receptors. Pharmacol. Rev. *54*, 161–202.

Idris, A.I., van 't Hof, R.J., Greig, I.R., Ridge, S.A., Baker, D., Ross, R.A., and Ralston, S.H. (2005). Regulation of bone mass, bone loss and osteoclast activity by cannabinoid receptors. Nat. Med. *11*, 774–779.

Idris, A.I., Rojas, J., Greig, I.R., Van't Hof, R.J., and Ralston, S.H. (2008a). Aminobisphosphonates cause osteoblast apoptosis and inhibit bone nodule formation in vitro. Calcif. Tissue Int. *82*, 191–201.

Idris, A.I., Sophocleous, A., Landao-Bassonga, E., van't Hof, R.J., and Ralston, S.H. (2008b). Regulation of bone mass, osteoclast function and ovariectomy-induced bone loss by the type 2 cannabinoid receptor. Endocrinology *149*, 5619–5626.

Justesen, J., Stenderup, K., Ebbesen, E.N., Mosekilde, L., Steiniche, T., and Kassem, M. (2001). Adipocyte tissue volume in bone marrow is increased with aging and in patients with osteoporosis. Biogerontology *2*, 165–171.

Justesen, J., Stenderup, K., Eriksen, E.F., and Kassem, M. (2002). Maintenance of osteoblastic and adipocytic differentiation potential with age and osteoporosis in human marrow stromal cell cultures. Calcif. Tissue Int. *71*, 36–44.

Kong, Y.Y., Yoshida, H., Sarosi, I., Tan, H.L., Timms, E., Capparelli, C., Morony, S., Oliveira-dos-Santos, A.J., Van, G., Itie, A., et al. (1999). OPGL is a key regulator of osteoclastogenesis, lymphocyte development and lymph-node organogenesis. Nature *397*, 315–323.

Ledent, C., Valverde, O., Cossu, G., Petitet, F., Aubert, J.F., Beslot, F., Böhme, G.A., Imperato, A., Pedrazzini, T., Roques, B.P., et al. (1999). Unresponsiveness to cannabinoids and reduced addictive effects of opiates in CB1 receptor knockout mice. Science *283*, 401–404.

Lips, P., Courpron, P., and Meunier, P.J. (1978). Mean wall thickness of trabecular bone packets in the human iliac crest: changes with age. Calcif. Tissue Res. *26*, 13–17.

Merkouris, M., Mullaney, I., Georgoussi, Z., and Milligan, G. (1997). Regulation of spontaneous activity of the delta-opioid receptor: studies of inverse agonism in intact cells. J. Neurochem. *69*, 2115–2122.

Meunier, P., Aaron, J., Edouard, C., and Vignon, G. (1971). Osteoporosis and the replacement of cell populations of the marrow by adipose tissue. A quantitative study of 84 iliac bone biopsies. Clin. Orthop. Relat. Res. *80*, 147–154.

Ofek, O., Karsak, M., Leclerc, N., Fogel, M., Frenkel, B., Wright, K., Tam, J., Attar-Namdar, M., Kram, V., Shohami, E., et al. (2006). Peripheral cannabinoid receptor, CB2, regulates bone mass. Proc. Natl. Acad. Sci. USA *103*, 696–701.

Pertwee, R.G. (1999). Pharmacology of cannabinoid receptor ligands. Curr. Med. Chem. *6*, 635–664.

Raisz, L.G. (2005). Pathogenesis of osteoporosis: concepts, conflicts, and prospects. J. Clin. Invest. *115*, 3318–3325.

Ravinet, T.C., Delgorge, C., Menet, C., Arnone, M., and Soubrié, P. (2004). CB1 cannabinoid receptor knockout in mice leads to leanness, resistance to diet-induced obesity and enhanced leptin sensitivity. Int. J. Obes. Relat. Metab. Disord. *28*, 640–648.

Reusch, J.E., Colton, L.A., and Klemm, D.J. (2000). CREB activation induces adipogenesis in 3T3-L1 cells. Mol. Cell. Biol. *20*, 1008–1020.

Riggs, B.L., Wahner, H.W., Seeman, E., Offord, K.P., Dunn, W.L., Mazess, R.B., Johnson, K.A., and Melton, L.J., III. (1982). Changes in bone mineral density of the proximal femur and spine with aging. Differences between the postmenopausal and senile osteoporosis syndromes. J. Clin. Invest. *70*, 716–723.

Rzonca, S.O., Suva, L.J., Gaddy, D., Montague, D.C., and Lecka-Czernik, B. (2004). Bone is a target for the antidiabetic compound rosiglitazone. Endocrinology *145*, 401–406.

Stewart, T.L., Roschger, P., Misof, B.M., Mann, V., Fratzl, P., Klaushofer, K., Aspden, R.M., and Ralston, S.H. (2005). Association of COLIA1 Sp1 alleles with defective bone nodule formation in vitro and abnormal bone mineralisation in vivo. Calcif. Tissue Int. *77*, 113–118.

Tam, J., Trembovler, V., Di Marzo, V., Petrosino, S., Leo, G., Alexandrovich, A., Regev, E., Casap, N., Shteyer, A., Ledent, C., et al. (2008). The cannabinoid CB1 receptor regulates bone formation by modulating adrenergic signaling. FASEB J. *22*, 285–294.

Tintut, Y., Parhami, F., Le, V., Karsenty, G., and Demer, L.L. (1999). Inhibition of osteoblast-specific transcription factor Cbfa1 by the cAMP pathway in osteoblastic cells. Ubiquitin/proteasome-dependent regulation. J. Biol. Chem. *274*, 28875–28879.

van't Hof, R.J. (2003). Osteoclast formation in the mouse coculture assay. In Bone Research Protocols, M.H. Helfrich and S.H. Ralston, eds. (Totowa: Humana Press), pp. 145–152.

Verma, S., Rajaratnam, J.H., Denton, J., Hoyland, J.A., and Byers, R.J. (2002). Adipocytic proportion of bone marrow is inversely related to bone formation in osteoporosis. J. Clin. Pathol. *55*, 693–698.

Yajima, Y., Akita, Y., and Saito, T. (1986). Pertussis toxin blocks the inhibitory effects of somatostatin on cAMP-dependent vasoactive intestinal peptide and cAMP-independent thyrotropin releasing hormone-stimulated prolactin secretion of GH3 cells. J. Biol. Chem. *261*, 2684–2689.

Yang, D.C., Tsay, H.J., Lin, S.Y., Chiou, S.H., Li, M.J., Chang, T.J., and Hung, S.C. (2008). cAMP/PKA regulates osteogenesis, adipogenesis and ratio of RANKL/OPG mRNA expression in mesenchymal stem cells by suppressing leptin. PLoS ONE *3*, e1540.